Structural Engineering and Mechanics, *Vol. 74, No. 5 (2020) 601-609*
DOI: https://doi.org/10.12989/sem.2020.74.5.601

Investigation the fracture behavior of high-density polyethylene PE80 weakened by inclined U-notch with end hole

Saeed Soltaninezhad[1,2], Ataallah Soltani Goharrizi[1] and Hadi Salavati*[3]

[1]Department of Chemical Engineering, Shahid Bahonar University of Kerman, Kerman, Iran
[2]Kerman Gas Company, Kerman, Iran
[3]Department of Mechanical Engineering, Shahid Bahonar University of Kerman, Kerman, Iran

(Received April 8, 2019, Revised January 3, 2020, Accepted January 10, 2020)

Abstract. In this article, the Strain Energy Density (SED) averaged over a well-defined control volume at a notch edge was applied in combination with the Equivalent Material Concept (EMC) to assess the fracture behaviors of some keyhole-notched specimens made of a High-Density Polyethylene (HDPE-PE80) material under mixed-mode loading conditions. An experimental program was performed and 54 new experimental data were totally provided. Additionally, different loading mode ratios were regarded by changing the inclination angles of the notches with respect to the applied load directions. The results obtained from the determined criteria were in good agreement with those of the experimental data.

Keywords: HDPE- PE80; ductile failure; keyhole notch; loading mode ratio

1. Introduction

The high density polyethylene (HDPE) has been used in pipe manufacturing for over 50 years in sectors of water distribution, sewer systems, and gas distribution (Frank 2009). features of HDPE pipe are, leak free, corrosion, abrasion and chemical resistant, excellent flow characteristics, lightweight and flexible, ductility and toughness. the HDPE is marketed on PE63, PE80 and PE100. the PE80 resin was developed at end of the '70s and has been widely used to produce pressure pipes in the water and gas industry. Nevertheless, Stress Cracking (SC) has been a major concern for PE80 pipes (Frank 2009). Therefore, investigations of PE80 fracture and serviceability have become highly important.

PE80 is a semi-crystalline thermoplastic material with a ductile behavior. The rules of Linear Elastic Notch Fracture Mechanics (LENFM) are no longer valid for ductile materials since they undergo significant plastic deformations when involved in the failure triggered by stress raisers. Alternatively, such well-known methods as the J-integral analysis, Crack-Tip Opening Displacement (CTOD) test, Crack-Tip Opening Angle (CTOA) measurement, and Resistance-curve (R-curve) approach have been utilized to analyze the fracture toughness of ductile elements subjected to cracks and notches (Anderson 1995).

Some experimental research conducted on specimens with notches made of aluminum alloys EN-AW 2024, it follows that the normal stress vector component on the critical plane determines the fracture. This plane, in the case of tensile specimens with notches, is perpendicular to the load direction. It is shown that the value of the critical normal stress dependents on the maximal plastic shear strains and the accumulated damage (and material weakening) occurs faster on the free surface than on the inside of the material (Derpeński and Seweryn 2016).

In this regard, any typical structural elements are commonly involved in varied types of notches, including U-, V-, VO-, and keyhole notches, which can result in the weakening of their structural strengths as caused by the stress concentration around the notch tip. Many researches have investigated in the recent and past literatures the fracture behaviour of pointed and blunt notches under pure or prevalent mode I loading (Gogotsi 2003, Nui *et al*. 1994, Seweryn 1994, Strandberg 2002). In some contribution, the stress filed around the notch tips has been already studied (Irwin 1957, Mori 1964, Creager and Paris 1967, Atzori *et al*. 1997, Lazzarind Tovo 1996, Filippi *et al*. 2002, Zappalorto and Lazzarin 2011).

The brittle or quasi-brittle fractures of notched components can be predicted via several proposed fracture criteria, such as maximum circumferential stress criterion, Mean Stress (MS) criterion, Imaginary Crack Method (ICM), Finite Fracture Mechanics (FFM), and averaged Strain Energy Density (SED) criterion. SED is a most accurate criterion for predicting the static fracture of notched members and is based on the evaluation of an averaged SED over a control volume under the different mode I, mixed-mode, and torsion loading conditions (Salavati *et al*. 2018, Behnam Saboori *et al*. 2018, Torabi and berto 2014).

As stated by this criterion, the occurrence of a static fracture is dependent on the critical SED value averaged over a well-defined control volume. The control volume depends on the material characteristics and notch geometries, including fracture toughness, ultimate tensile strength, notch angle, and Poisson coefficient. The critical SED depends on the material characteristics of ultimate

*Corresponding author, Assistant Professor
E-mail: hadi_salavati@uk.ac.ir

http://www.techno-press.com/journals/sem&subpage=7
ISSN: 1225-4568 (Print), 1598-6217 (Online)

tensile strength and Young's modulus (Lazzarin and Zambardi 2001, Lazzarin and Berto 2005, Berto and Lazzarin 2014, Lazzarin *et al*. 2013). Many investigations have been done to evaluate the static failure of brittle or quasi-brittle notched materials like polymethyl-methacrylate (Berto *et al*. 2012), polycrystalline graphite (Salavati *et al*. 2018, Torabi and Berto 2014), and ceramics (Wang *et al*. 1992) according to the SED criterion. Recently, this theory has been developed to assess the fractures occurred to functionally graded materials (Salavati *et al*. 2014a, b 2015a, b,c, 2017, Mohammadi *et al*. 2017a,b,c,d, Mosaddeghi *et al*. 2017). The possibility of highly accurate calculation of SED mean value over a control volume through coarse meshes by using Finite Element (FE) models can be regarded as a major advantage of this criterion (Lazzarin *et al*. 2010, Campagnolo *et al*. 2016). Although the mentioned criterion can be used to predict the brittle or quasi-brittle fractures of notched components, any applied materials must be typically engineered as ductile structures like those of metallic materials, including steel alloy and aluminum and titanium alloy, as well as polymers or polymer-based composites, most of which may contain notches of various shapes (Campagnolo *et al*. 2016). Moreover, the 3d effect on fracture has been investigated by the many researches (Pook *et al*. 2015, Zappalorto and Lazzarin 2001).

Two of the first attempts to utilize elastic analysis instead of elastic–plastic one has been made by Glinka and Molski (1981), and Glinka (1985) They made use of the strain energy density (SED) approach to determine the elastic–plastic stress distribution around some notched components. In their works, first, the elastic stress concentration factor has been used to formulate the elastic stresses at the notch tip and then, the SED at the notch tip has been equated for elastic and elastic–plastic components with the aim to determine the stress distribution in the notched component made of ductile material. With the aim of applying both the TCD and the SED to nonlinear-elastic conditions, but keeping their simple linear-elastic formulation, both approaches will be combined with the Equivalent Material Concept (EMC) (Torabi and Berto 2016, Torabi and Alaei 2015). Based on the EMC, the SED criterion assumes that the areas under the stress-strain curves in uniaxial tension are equal for ductile and virtual brittle materials with similar moduli of elasticity and fracture toughness (Torabi 2015, 2013).

The main purposes of the present paper are as follows:

- The well-known SED criterion was employed in combination with the Equivalent Material Concept (EMC) to predict the fracture behavior in O-notched ductile components without the need for performing any experiments or an elastic-plastic analysis.
- A new set of experimental data can be provided by O-notched specimens made of HDPE-PE80 with different values of notch inclination angles, which can be useful to engineers engaged with the static strength analysis of PE80 components.

In the first part of the paper, the description of the experimental program is carried out. The second part summarises the SED criterion, the SED combination with the Equivalent Material Concept (EMC) and describes the numerical models used to evaluate the local SED. The third part reports the final synthesis from key-hole notches as a function of the averaged SED.

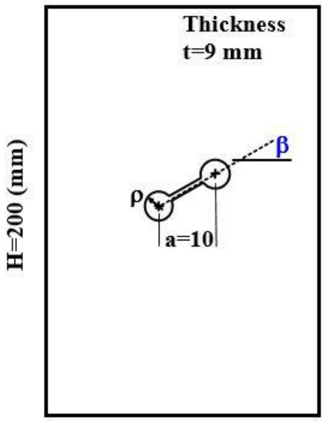

Fig. 1 The geometries of the inclined U-notch with end hole specimens

2. Fracture experiments

2.1 Materials and geometries

In this study, a commercial PE80 material was taken from a 160-mm SDR11 gas pipe. Table 1 summarizes the standard test method, the test conditions and the main material properties experimentally examined in our lab. The experimental specimens were weakened by using an eccentric double keyhole notch as shown in Fig. 1. For all the specimens, the length (H), the width (W) and the thickness of the specimens were selected 200, 45 and 9 mm, respectively. Moreover, the distance between the notch centers was selected 10mm. The effects of the notch tip radius, ρ, and its inclination angle, β, on the fractures of the specimens under the tensile loads were investigated. Upon varying the inclination angle, various loading mode ratios could be produced. 3 values of the notch radius (ρ=0.5, 1, and 2 mm) and 6 values of the angle (β=0°, 15°, 30°, 45°, 60°, and 75°) were considered for the test specimens. Fig. 2 portrays some images of the specimens and details of the notches.

2.2 Experimental procedure

First, some plates of 9-mm thickness were obtained from PE80 gas pipe grades to prepare the test specimens (Fig. 1). The mentioned thickness was selected to provide the strain conditions of the planes at the notch tips. Then, the specimens were accurately fabricated by using a Computer Numerically Controlled (CNC) machine tool spindle that equipped with a water cooler for minimum temperature effect on the specimens. The fracture tests were performed by using a universal tension-compression test machine under displacement control with the constant displacement rate of 5 mm/min. In total, 54 mixed-mode

Table 1 Mechanical properties of HDPE PE-80

Material property	Value	Test method	condition
Modulus E_y, MPa	176	ISO 6259-3	25 mm/min, 25^0C
Modulus $E_{1\%}$, MPa	827	ISO 6259-3	25 mm/min, 25^0C
modulus $E_{2\%}$, MPa	625	ISO 6259-3	25 mm/min, 25^0C
Ultimate tensile strength, MPa	19.8	ISO 6259-3	25 mm/min, 25^0C
Elongation at peak %	11.2	ISO 6259-3	25 mm/min, 25^0C
Elongation at break %	585	ISO 6259-3	25 mm/min, 25^0C
Fracture toughness, MPa $m^{0.5}$	2.35	ASTM E399-81	Bend test,5 mm/min, 25^0C
Poisson's ratio, ν	0.4	ASTM E 132	25^0C
Density, kg/m^3	957	EN 1183-1/2	23^0C,
Carbon black %	2.5	ISO 6964	550-600 ^{0}C

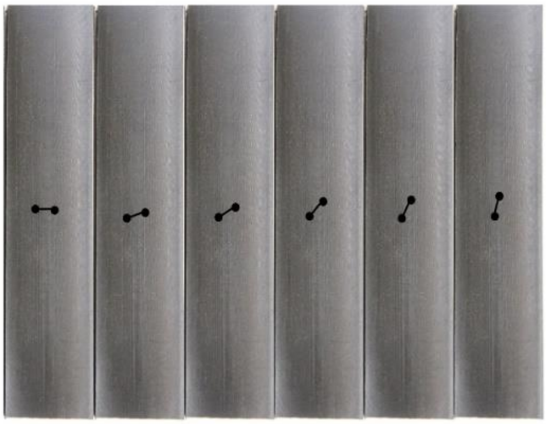

Fig. 2 The different eccentric double keyhole notched specimens: β=0°,15°, 30°, 45°, 60°, and 75° and ρ=2 mm

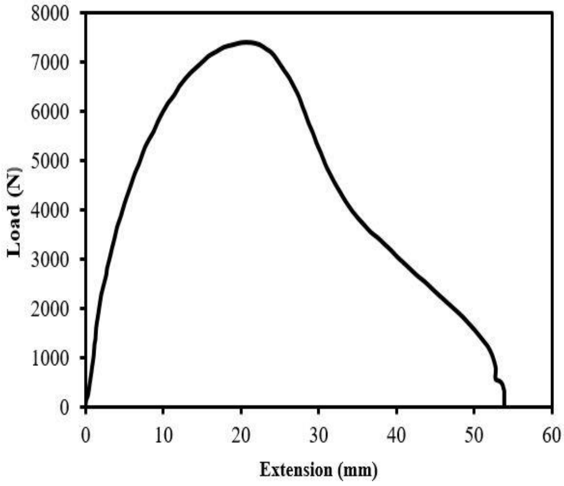

Fig. 3 Load-extension curves for the double keyhole notched specimens: β=45° and ρ=1 mm

Fig. 4 The broken inclined U-notch with end hole specimens: (a) β=75° and ρ=2 mm

fracture tests with 3 iterations were conducted. The load-extension curves for the double keyhole notched specimens were used to determine the critical fracture loads. Fig. 3 displays the related curves for the mentioned specimens in the cases of ρ=2 mm and β=0°. Fig. 4 shows some broken inclined U-notch with end hole specimens.

The values of the fracture loads and their corresponding mean values (F) are presented in Table 2. As evident, the fracture load enhances by decreasing the notch radius and increasing the inclination angle.

3. Evaluation of the loading mode ratio parameter

To quantify the loading mode ratio in the simulated specimens, FE analysis was performed. The definitions of the generalized Notch-Stress Intensity Factors (N-SIFs) for the mode I and mode II problems are respectively as follows (Zappalorto and Lazzarin 2011):

$$K_{I.\rho} = \frac{2\sqrt{2\pi r}(\sigma_{\theta\theta})_{\theta=0}}{[2 + 1.25\left(\frac{\rho}{r}\right) + 1.5\left(\frac{\rho}{r}\right)^2 + 1.25\left(\frac{\rho}{r}\right)^3]} \quad (1)$$

$$K_{II.\rho} = \frac{\sqrt{2\pi r}(\tau_{r\theta})_{\theta=0}}{[2 + 1.625\left(\frac{\rho}{r}\right) + 0.75\left(\frac{\rho}{r}\right)^2 + 1.875\left(\frac{\rho}{r}\right)^3]} \quad (2)$$

where $\sigma_{\theta\theta}$ and $\tau_{r\theta}$ are the stresses at distance r from the local frame origin. Eqs.(2) – (3) only provide slight variations, but not a constant value for the N-SIF. In (Atzori *et al.* 2005, Berto *et al.* 2012), a wide investigation of the

Table 2 Experimental data of PE80

0	B^0	ρ mm	F_1,N	F_2,N	F_3,N	$F_{average}$
1	75	0.5	8011.80	8199.20	8145.70	8119
2	75	1	7600.80	7803.30	7759.20	7721
3	75	2	7788.10	7524.70	7441.80	7585
4	60	0.5	7730.3	7848.9	7511	7697
5	60	1	6865.5	7720.4	7695.4	7427
6	60	2	7353	6987.6	7248.1	7196
7	45	0.5	7685.6	7168.6	7706.2	7520
8	45	1	7423.7	7262.8	6951.3	7213
9	45	2	6800.7	7206.9	6833.6	6947
10	30	0.5	7232.4	7032.3	7355	7207
11	30	1	6986.6	7016.1	6684.5	6896
12	30	2	6522.6	6675.2	6395.1	6531
13	15	0.5	7217.7	7334.4	7307.4	7287
14	15	1	6798.8	6959.2	6708	6822
15	15	2	6313.2	6467.2	6634.9	6472
16	0	0.5	7045	6984.7	6885.10	6972
17	0	1	6516.2	6819.4	6857.1	6731
18	0	2	6056.60	6127.8	6085.1	6090

Table 3 The loading mode ratios of the studied geometries

β^0	ρ, mm	$\overline{K}_{II.\rho}/\overline{K}_{I.\rho}$	χ
0	2	0.17	0.1
15	2	0.28	0.2
30	2	0.21	0.1
45	2	0.17	0.1
60	2	0.16	0.1
75	2	0.18	0.1
0	1	0.47	0.3
15	1	0.55	0.3
30	1	0.03	0.0
45	1	0.63	0.4
60	1	0.48	0.3
75	1	0.35	0.2
0	0.5	0.40	0.2
15	0.5	0.38	0.2
30	0.5	0.34	0.2
45	0.5	0.38	0.2
60	0.5	0.43	0.3
75	0.5	0.33	0.2

slightly oscillating trends of notch tips has been presented. The mean values of the generalized NSIFs can be calculated by respectively defining the following expressions in the above-mentioned modes so as to avoid any weak dependence on the notch tip distance (Lazzarin and Filippi 2006):

$$\overline{K}_{I.\rho} = \frac{1}{\eta\rho}\int_{r_0}^{r_0+\eta\rho}(K_{I.\rho})dr \tag{3}$$

$$\overline{K}_{II.\rho} = \frac{1}{\eta\rho}\int_{r_0}^{r_0+\eta\rho}(K_{II.\rho})dr \tag{4}$$

where η has been set between 0.2 and 0.3 (Lazzarin and Zambardi 2001) (0.25) in this study.

The loading mode ratio can be evaluated based on the following definition (Lazzarin and Filippi 2006):

$$\chi = \frac{2}{\pi}arctan\left(\frac{\overline{K}_{I.\rho}}{\overline{K}_{II.\rho}}\right) \tag{5}$$

The values of the loading mode ratio (χ) are equal to 0 and 1 under the loading conditions of pure modes I and II, respectively. The values of $\frac{\overline{K}_{I.\rho}}{\overline{K}_{II.\rho}}$ and χ related to the simulated specimens are calculated and summarized in Table 3.

4. Application of the SED criterion with the EMC

In this paper, the EMC as a novel concept was employed to equate the ductile and virtual brittle materials from the SED viewpoint. The EMC provides an imaginary consideration of a virtual brittle instead of a ductile material to investigate a linear elastic rather than an elastic-plastic behavior in fractures. The simple criteria for brittle fractures could be ultimately utilized in the study of the fracture phenomenon occurring to ductile materials.

Based on the EMC, the SED values of the existing virtual brittle and ductile materials with similar moduli of elasticity could be assumed to be the same. SED actually represents the strain energy absorbed by the unit volume of a material. The following equation can be written for a ductile material undergoing a significant plastic deformation based on the power-law relationship of the strain-hardening coefficient and exponent in the plastic zone:

$$\sigma = K\varepsilon_\sigma^n \tag{6}$$

where σ and ε_σ indicate the plastic stress and strain, respectively. The parameters of K and n demonstrate the strain-hardening coefficient and exponent, which depend on the material properties, respectively. Fig. 5 depicts a schematic representation of a tensile stress-strain curve for a typical ductile material, in which E, Y, u, and ε_f denote the elastic modulus, yield strength, ultimate tensile strength, and strain at rupture, respectively. The total SED can be expressed in the following general elastic-plastic form:

$$(SED)_{tot} = (SED)_e + (SED)_p \tag{7}$$

As defined in the EMC, the equivalent virtual brittle material has the same values of E and K_{Ic} respectively representing the elastic modulus and plane-strain fracture toughness, but an undetermined value of the ultimate tensile strength. In Fig. 6, a typical uniaxial stress-strain curve is schematically shown for the virtual brittle material, in which the parameters of ε^*_f and σ^*_f stand for the strain

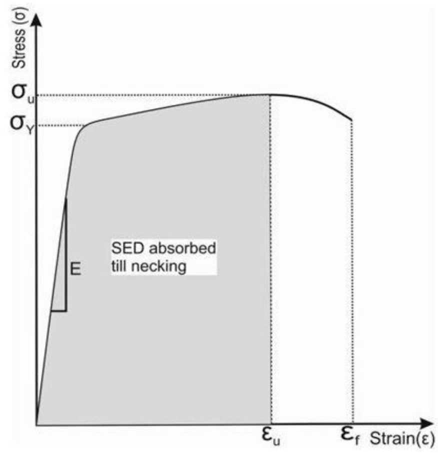

Fig. 5 A typical tensile stress-strain curve for a sample ductile material (Torabi 2013)

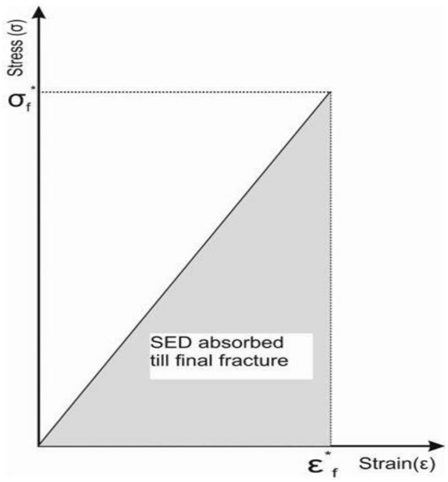

Fig. 6 A typical uniaxial stress-strain curve for a sample virtual brittle material (Torabi 2013)

(final fracture) occurring with the crack initiation due to the brittleness and the ultimate tensile strength, respectively. Upon the crack initiation, the SED for this material can be calculated as follows:

$$(\mathrm{SED})\mathrm{EMC} = \frac{\sigma_f^{*\,2}}{2E} \tag{8}$$

Assuming the equality of the SED values for both the virtual brittle and real ductile materials according to the EMC, we have:

$$(\mathrm{SED})\mathrm{tot} = \frac{\sigma_f^{*\,2}}{2E} \tag{9}$$

$$\sigma_f^* = \sqrt{2E(SED)_{tot}} \tag{10}$$

The parameter of σ_f^* presented in Eq. (11) can be used together with the material fracture toughness (K_{Ic} or K_I) as the two necessary inputs of different brittle fracture criteria for predicting crack initiation from notches in ductile members subjected to tension (pure mode I loading condition (Campagnolo *et al*. 2016, Torabi 2013).

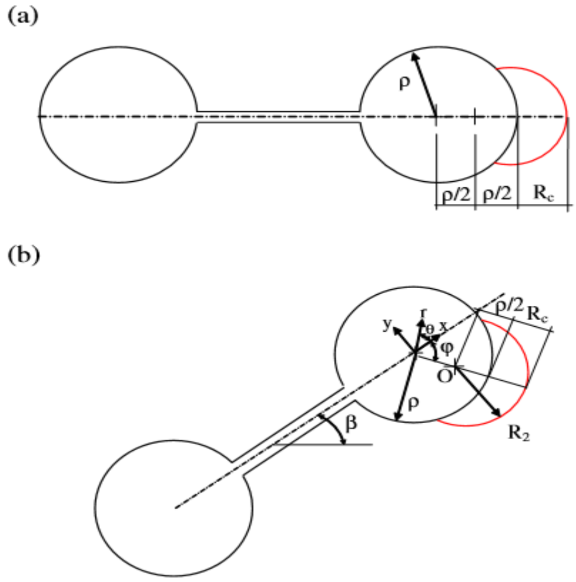

Fig. 7 The control volumes in the keyhole notched specimens under (a) mode I and (b) mixed-mode conditions (Salavati *et al*. 2018)

Lazzarin and Zambardi (2001 states that brittle or quasi-brittle failure in an unnotched material, Wc, occurs when the SED averaged over a control volume becomes equal to the critical SED. The SED approach depends on the precise control volume definition, but not on the notch sharpness. This method was first applied to sharp V-notches with a zero radius and then extended to blunt V- and U-notches under a mode I loading condition (Lazzarin and Berto 2005).

Under the above-mentioned loading condition, the critical control volume in keyhole notched specimens is centered proportionate to the notch bisector line (Fig. 7(a)). However, under a mixed-mode loading condition, the volume is centered along the edge instead of the tip of the notch, i.e., on the point of maximal principal stress (Fig. 7(b)) (Berto *et al*. 2007).

The control radius (R_C) as a function of fracture toughness (K_{IC}), ultimate tensile strength (σ_{ut}), and Poisson's ratio (v) of the material are expressed as follows (Anderson 1995, Yosibash *et al*. 2004):

$$R_C = \frac{(1+\nu)(5-8\nu)}{4\pi}\left(\frac{K_{IC}}{\sigma_{ut}}\right)^2 \tag{11}$$

The SED critical value can be calculated as follows:

$$W_C = \frac{\sigma_{ut}^2}{2E} \tag{12}$$

where σ_{ut} and E are the ultimate tensile strength and Young's modulus of the material, respectively (Anderson 1995, Yosibash *et al*. 2004).

In the present work, the value of W_c was considered to be 2.33 J/m3, which was the SED average (surface under the stress-strain curve before the yield point) for PE80.

The FE code of ABAQUS 6.14 was applied to create 2 models for each geometry, one model for determining the

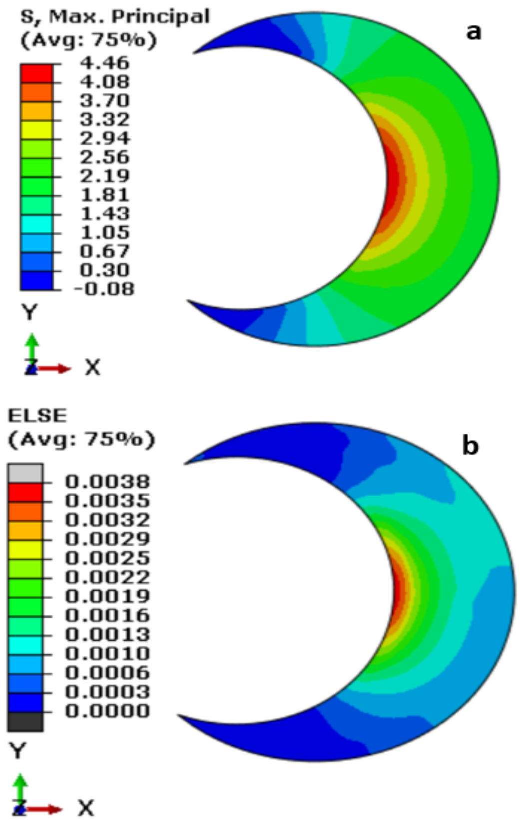

Fig. 8 (a)The maximal principal stress and (b) SED contour lines for the configuration of ρ=2 mm and β=45°

Table 4 Comparison between numerical and experimental data

β^0	P ,mm	F_{exp} ,N	F_{FEM} ,N	F_{FEM}/F_{exp}	ϕ^0
0	2	6090	5111	0.84	0.6
15	2	6472	5182	0.80	17.1
30	2	6531	5374	0.82	32.0
45	2	6947	5677	0.82	46.4
60	2	7196	6193	0.86	62.7
75	2	7585	7210	0.95	77.8
0	1	6731	5862	0.87	0.0
15	1	6822	5931	0.87	17.0
30	1	6822	5931	0.87	31.4
45	1	7213	6706	0.93	50.4
60	1	7427	7545	1.02	60.0
75	1	7721	8855	1.15	76.9
0	0.5	6972	6117	0.88	0.0
15	0.5	7287	6157	0.84	17.0
30	0.5	7207	6415	0.89	33.3
45	0.5	7520	6955	0.92	49.7
60	0.5	7697	7990	1.04	60.0
75	0.5	8119	9657	1.19	77.1

point of maximal principal stress and the other one for obtaining the averaged SED over the well-defined control volume. All the analyses were based on the linear-elastic hypotheses under plane strain conditions. Fig. 8 illustrates the maximal principal stress and SED contour lines for a configuration with ρ=2 mm and β=45°.

The values of the crack initiation angle ($\varphi°$) are summarized in the last column of Table 4. The critical fracture load could be evaluated by determining the SED mean value over the control volume using the following expression:

$$\frac{F_{ap}}{F_{cr}} = \sqrt{\frac{\overline{W}_{ap}}{W_{cr}}} \tag{13}$$

where $F_{ap}$is the applied load, F_{cr}, $\overline{W}_{ap}$, and W_{cr} indicate the applied and critical fracture loads, the SED averaged over the control volume relevant to F_{ap}, is the critical SED, respectively (Salavati *et al*. 2018). The summarized values of the critical fracture load presented in Table 4 show good agreement with the experimental data.

Fig. 9 (a)-(f) displays the experimental results, as well as the theoretical predictions for each inclination angle value obtained from the notch root radius based on the SED approach. It is important to note that for all the cases, there was very good agreement between the theoretical and experimental values. Moreover, the average deviation between the theoretical and experimental values of the critical fracture loads was found to be about 15%.

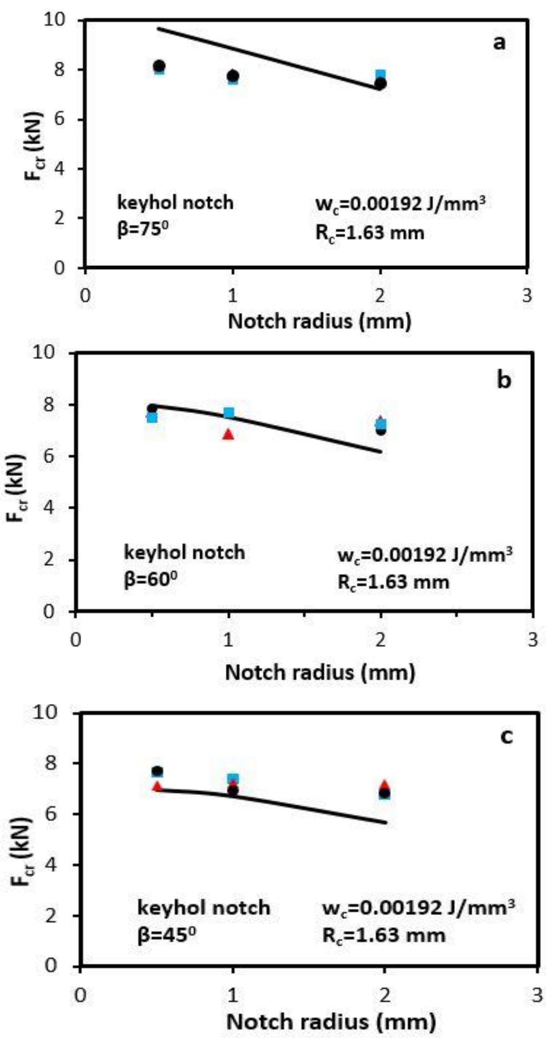

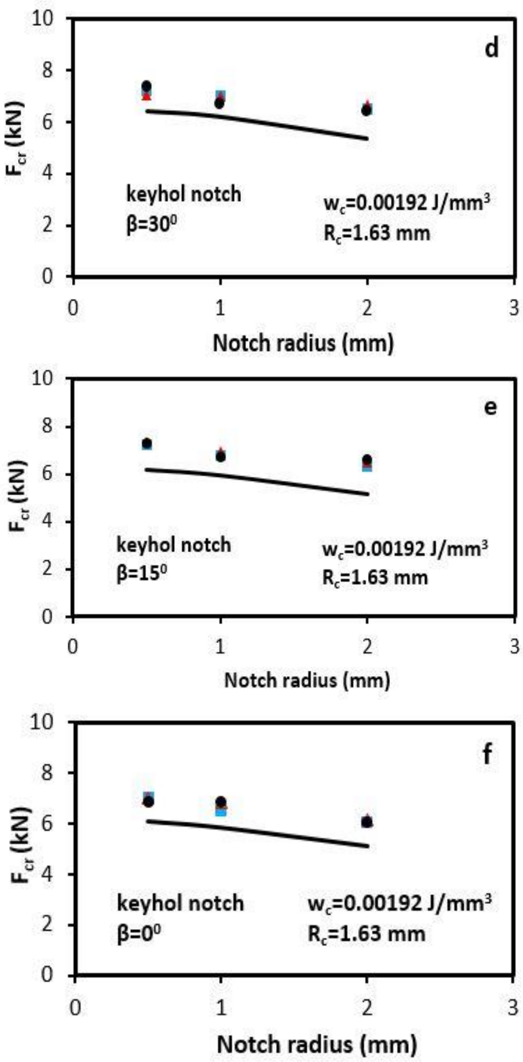

Fig. 9 The critical loads based on notch radius for the notch angle inclinations of (the solid line represents the SED-based fracture assessment)

5. Conclusion

In the present work, the SED averaged over a well-defined control volume ahead at the notch edge was utilized to obtain the critical fracture loads of the keyhole notched specimens made of PE80 under a mixed-mode loading condition.

The main results of this investigation are summarized as follows:

1. The SED criterion in combination with the EMC model provided a suitable approach to the prediction of the ductile fracture behavior of PE80.

2. The limited average deviation (15%) between the theoretical and experimental values based on the critical fracture loads indicated the model's accuracy.

References

Anderson, L. (1995), *Fracture Mechanics: Fundamentals and Applications*, 2nd ed., CRC Press LLC, Florida.

Atzori, B., Filippi, S., Lazzarin, P. and Berto, F. (2005), "Stress distributions in notched structural components under pure bending and combined traction and bending", *Fatigue Fract. Eng. Mater. Struct.*, **28**, 13-23. https://doi.org/10.1111/j.1460-2695.2004.00831.x.

Atzori, B., Lazzarin, P. and Tovo, R. (1997), "Stress distributions for V-shaped notches under tensile and bending loading", *Fract. Eng. Mater. Struct.*, **20**, 1083-1092. https://doi.org/10.1111/j.1460-2695.1997.tb00314.x.

Behnam S., Torabi, A.R., Berto, F. and Razavi, S.M.J. (2018), "Averaged strain energy density to assess mixed mode I/III fracture of U-notched GPPS samples", *Struct. Eng. Mech.*, **65**(6), 699-706. https://doi.org/10.12989/sem.2018.65.6.699.

Berto, F. and Lazzarin, P. (2014), "Recent developments in brittle and quasi-brittle failure assessment of engineering materials by means of local approaches", *Mater. Sci. Eng. R. Rep.*, **75**, 1-48. https://doi.org/10.1016/j.mser.2013.11.001/

Berto, F., Elices, M., Lazzarin, P. and Zappalorto, M. (2012), "Fracture behaviour of notched round bars made of PMMA subjected to torsion at room temperature", *Eng. Fract. Mech.*, **90**, 143-160. https://doi.org/10.1016/j.engfracmech.2012.05.001.

Berto, F., Lazzarin, P. and Radaj, D. (2012), "Fictitious notch rounding concept applied to V-notches with root holes subjected to in-plane shear loading", *Eng. Fract. Mech.*, **79**, 281-294. https://doi.org/10.1016/j.engfracmech.2011.11.007.

Berto, F., Lazzarin, P., Gómez, F. J. and Elices, M. (2007), "Fracture assessment of U-notches under mixed mode loading: two procedures based on the 'equivalent local mode I' concept", *Int. J. Fract.*, **148**, 415-433. https://doi.org/10.1007/s10704-008-9213-7.

Campagnolo, A., Meneghetti, G. and Berto, F. (2016), "Rapid finite element evaluation of the averaged strain energy density of mixed-mode (I + II) crack tip fields including the T-stress contribution", *Fatigue Fract. Eng. Mater. Struct.*, **39**, 982-998. https://doi.org/10.1111/ffe.12439.

Creager, M. and Paris, P.C. (1967), "Elastic field equations for blunt cracks with reference to stress corrosion cracking", *Int. J. Fract.*, **3**, 247-252. https://doi.org/10.1007/BF00182890.

Filippi, S., Lazzarin, P. and Tovo, R. (2002), "Developments of some explicit formulas useful to describe elastic stress fields ahead of notches in plates", *Int. J. Solids. Struct.*, **39**, 4543-4565. https://doi.org/10.1016/S0020-7683(02)00342-6.

Frank, A. and Pinter, G. and Lang, R.W. (2009), "Prediction of the remaining lifetime of polyethylene pipes after up to 30 years in use", *Polym. Test.*, **28**, 737-745. https://doi.org/10.1016/j.polymertesting.2009.06.004.

Glinka, G. (1985), "Energy density approach to calculation of inelastic strain-stress near notches and cracks", *Engng. Fract. Mech.*, **22**, 485-508. https://doi.org/10.1016/0013-7944(85)90148-1.

Glinka, G., Molski, K. (1981), "A method of elastic-plastic stress and strain calculation at a notch root", *Mater. Sci. Engng*. **50**, 93-100. https://doi.org/10.1016/0025-5416(81)90089-6.

Gogotsi, G. A. (2003), "Fracture toughness of ceramics and ceramic composites", *Ceram. Int.*, **29**, 777-784. https://doi.org/10.1016/S0272-8842(02)00230-4.

Irwin, G.R., (1957), "Analysis of stresses and strain near the end of a crack transversing a plate", *J. Appl. Mech.*, **24**, 361- 364.

Knésl, Z. (1991), "A criterion of V-notchstability", *Int. J. Fract*, **48**, R79-R83.

Lazzarin, P. and Berto, F. (2005), "Some expressions for the strain energy in a finite volume surrounding the root of blunt V-notches", *Int. J. Fract.*, **135**, 161-185. https://doi.org/10.1007/s10704-005-3943-6.

Lazzarin, P. and Berto, F. (2005), "Some expressions for the strain energy in a finite volume surrounding the root of blunt V-notches", *Int. J. Fract*., **135**, 161-185. https://doi.org/10.1007/s10704-005-3943-6.

Lazzarin, P. and Filippi, S. (2006), "A generalized stress intensity factor to be applied to rounded V-shaped notches", *Int. J. Solids Struct*., **43**, 2461-2478. https://doi.org/10.1016/j.ijsolstr.2005.03.007.

Lazzarin, P. and Tovo, R. (1996), "A unified approach to the evaluation of linear elastic stress fields in the neighborhood of cracks and notches", *Int. J. Fract*, **78**, 3-19. https://doi.org/10.1007/BF00018497.

Lazzarin, P. and Zambardi, R. (2001), "A finite-volume-energy based approach to predict the static and fatigue behavior of components with sharp V-shaped notches", *Int, J. Fract*., **112**, 275-298. https://doi.org/10.1023/A:1013595930617.

Lazzarin, P., Berto, F. and Ayatollahi, M R. (2013), "Brittle failure of inclined key-hole notches in isostatic graphite under in-plane mixed mode loading", *Fract. Eng. Mater. Struct*., **36**, 942-955. https://doi.org/10.1111/ffe.12057.

Lazzarin, P., Berto, F. and Zappalorto, M. (2010), "Rapid calculations of notch stress intensity factors based on averaged strain energy density from coarse meshes: theoretical bases and applications", *Int. J. Fatigue*., **32**, 1559-1567. https://doi.org/10.1016/j.ijfatigue.2010.02.017.

Zappalorto, M. and Lazzarin, P. (2011), "In-plane and out-of-plane stress field solutions for V-notches with end holes", *Int. J. Fract*., **168**, 167-180. https://doi.org/10.1007/s10704-010-9567-5.

Mohammadi, H., Salavati, H., Alizadeh, Y. and Berto, F. (2017), "Prevalent mode II fracture assessment of inclined U-notched specimens made of tungsten-copper functionally graded material", *Theor Appl. Fract. Mec*., **89**, 90-99. https://doi.org/10.1016/j.tafmec.2017.01.010.

Mohammadi, H., Salavati, H., Alizadeh, Y., Abdullah, A. and Berto, F. (2017), "Fracture investigation of U-notch made of tungsten-copper functionally graded materials by means of strain energy density", *Fatigue Fract. Eng. M*., **40**, 1984-1993. https://doi.org/10.1111/ffe.12616.

Mohammadi, H., Salavati, H., Alizadeh, Y., Berto, F. and Panin, S. V. (2017), "Fracture investigation of V-notch made of tungsten-copper functionally graded materials", *Phys, Mesomech*., **20**, 457-464. https://doi.org/10.1134/S1029959917040117.

Mohammadi, H., Salavati, H., Mosaddeghi, M. R., Yusefi, A. and Berto, F. (2017), "Local strain energy density to predict mixed mode I + II fracture in specimens made of functionally graded materials weakened by V-notches with end holes", *Theor. Appl. Fract. Mec*., **92**, 47-58. https://doi.org/10.1016/j.tafmec.2017.05.009.

Mori K (1964), "Tension of a semi-infinite plate with a circular hole connected to the straight edge by a slit", *Bull JSME*., **7**, 272-277. https://doi.org/10.1299/jsme1958.7.272.

Mosaddeghi, M.R., Salavati, H., Alizadeh, Y. and Abdullah, A. (2017), "Fracture investigation of U-notched specimen made of cooper- steel functionally graded material under mode I loading, Modares mechanical Engineering", **17**, 1-9.

Nui, L. S., Chehimi, C. and Pluvinage, G. (1994), "Stress field near a large blunted tip V-notch and application of the concept of the critical notch stress intensity factor (NSIF) to the fracture toughness of very brittle materials", *Eng. Fract. Mech*., **49**, 325-335. https://doi.org/10.1016/0013-7944(94)90262-3.

Pook, P., Campagnolo, A., Berto, F. and Lazzarin, P. (2015), "Coupled fracture mode of a cracked plate under anti-plane loading", *Eng. Fractc. Mech*., **134**, 391-403. https://doi.org/10.1016/j.engfracmech.2014.12.021.

Salavati, H. and Berto, F. (2013), "Prediction the Charpy impact energy of functionally graded steels", *Eng. Solid Mech*., **2**, 21-28.

Salavati, H., Alizadeh, Y. and Ayatollahi, M. R. (2018), "Fracture assessment of inclined double keyhole notches in isostatic graphite", *Phys. Mesomech*., **21**, 110-116. https://doi.org/10.24411/1683-805X-2018-11003.

Salavati, H., Alizadeh, Y. and Berto, F. (2014), "The mechanism-based strain gradient plasticity theory to model the hot deformation behavior of functionally graded steels", *Eng. Mech*., **51**, 627-641. https://doi.org/10.12989/sem.2014.51.4.627.

Salavati, H., Alizadeh, Y. and Berto, F. (2015), "Fracture assessment of notched bainitic functionally graded steels under mixed mode (I + II) Loading", *Phys. Mesomech*., **18**, 307-325. https://doi.org/10.1134/S1029959915040049.

Salavati, H., Alizadeh, Y. and Berto, F. (2015), "Local strain energy density applied to bainitic functionally graded steels plates under mixed mode (I+II) loading", *Acta. Metallurgica Sinica*., **28**, 164-172. https://doi.org/10.1007/s40195-014-0182-8.

Salavati, H., Alizadeh, Y., Kazemi, A. and Berto, F. (2015), "A new expression to evaluate the critical fracture load for bainitic functionally graded steels under mixed mode (I + II) loading", *Eng. Fail Anal*., **48**, 121-136. https://doi.org/10.1016/j.engfailanal.2014.11.005.

Salavati, H., Berto, F. and Alizadeh, Y. (2014), "The flow stress assessment of austenitic-martensitic functionally graded steel under hot compression", *Eng. Solid. Mech*., **2**, 83-90.

Salavati, H., Mohammadi, H., Yusefi, A. and Berto, F. (2017), "Fracture assessment of V-notched specimens with end holes made of tungsten-copper functionally graded material under mode I loading", *Theor. Appl. Fract. Mec*., 357-367. https://doi.org/10.1016/j.tafmec.2017.06.013.

Seweryn, A. (1994), "Brittle fracture criterion for structures with sharp notches", *Eng. Fract. Mech*., **47**, 673-681. https://doi.org/10.1016/0013-7944(94)90158-9.

Strandberg, M. (2002), "Fracture at V-notches with contained plasticity", *Eng. Fract. Mech*., **69**, 403-415. https://doi.org/10.1016/S0013-7944(01)00079-0.

Torabi, A. (2013), "The Equivalent Material Concept: Application to Failure of O-Notches", *Eng. Solid Mech*., **1**, 129-140.

Torabi, A. R, Habibi, R., Mohammad Hosseini, B. (2015), "On the Ability of the Equivalent Material Concept in Predicting Ductile Failure of U-Notches under Moderate- and Large-Scale Yielding Conditions", *Phys. Mesomech*., **18**, 337-347. https://doi.org/10.1134/S1029959915040062.

Torabi, A. R., Alaei, M. (2015), "Mixed-mode ductile failure analysis of V-notched Al7075-T6 thin sheets", *Eng. Fract. Mech*., **150**, 70-75. https://doi.org/10.1016/j.engfracmech.2015.10.037.

Torabi, A. R., and berto, F., (2014), "Mixed mode fracture assessment of U-notched graphite Brazilian disk specimens by means of the local energy", *Struct. Eng. Mech*., **50**(6), 723-740. https://doi.org/10.12989/sem.2014.50.6.723.

Torabi, A. R., Berto, F., Campagolo, A. (2016), "Elastic-plastic fracture analysis of notched Al7075-T6 plates by means of the local energy combined with the equivalent material concept", *Phys. Mesomech*., **19**, 204-214. https://doi.org/10.24411/1683-805X-2016-00049.

Torabi, R. and Berto, F. (2014), "Strain energy density to assess mode II fracture in U-notched disk-type graphite plates", *Int. J. Damage. Mech*., **23**, 917-930. https://doi.org/10.1177/1056789513519349.

Wang, J., Rainforth, W. M., Wadsworth, I. and Stevens R. (1992), "The effects of notch width on the SENB toughness for oxide ceramics", *J. Eur. Ceram. Soc*., **10**, 21-31. https://doi.org/10.1016/0955-2219(92)90115-T

Yosibash, Z., Bussiba, A. and Gilad, I. (2004), "Failure criteria for brittle elastic materials", *Int. J. Fract*., **125**, 307-333.

Zappalorto, M. and Lazzarin, P. (2011), "In-plane and out-of-plane stress field solutions for V-notches with end holes", *Int. J. Fract*., **168**, 167-180. https://doi.org/10.1007/s10704-010-9567-5.

CC

Nomenclature

HDPE	high density polyethylene
PE80	polyethylene grid 80
ν	Poisson's ratio
E	Young's modulus
χ	loading mode ratio
$\sigma\theta\theta$ and $\tau r\theta\theta$	stresses at Distance r from the local frame origin
σut	ultimate tensile strength
KI,ρ and KII,ρ	notch Stress Intensity Factor (SIF)
R	control radius
KIc	fracture toughness
Fcr	critical fracture load
Fap	applied load
SED	strain energy density
Wcr	critical SED
Wap	averaged SED over the related control volume